ELSEVIER

Electrical breakdown of human erythrocytes: a technique for the study of electro-haemolysis

Lyn D. Oliver[1], Hans G.L. Coster*

UNESCO Centre for Membrane Science and Technology and the Department of Biophysics, School of Physics, University of New South Wales, Sydney 2052, Australia

Abstract

This paper describes a technique suitable for investigating the electromechanical breakdown properties of erythrocyte cells. The cells were exposed to square wave electric pulses of precise duration and voltage. The erythrocytes were suspended in normal isotonic saline between two opposing platinum electrodes. A red LED light source and photodiode detector system were positioned orthogonally to the electrodes to record changes in the light transmission that occur immediately after applying an electric pulse. The light transmitted through the electrically treated erythrocyte suspension could be monitored continuously. Experiments were conducted to explore the inter-relationship between the critical voltage and pulse length for haemolysis. Human blood taken from "healthy" donors underwent haemolysis at a critical field strength of 304 kV/m for a 5 μs pulse and 292 kV/m for a 50 μs pulse. The relationship of critical pulse length and critical voltage for the blood samples was found to be inversely linear.
© 2003 Elsevier B.V. All rights reserved.

Keywords: Erythrocyte; Electrical breakdown; Haemolysis; Membrane

1. Introduction

A "reversible electrical breakdown" of cell membranes was first observed in current–voltage sweeps using intracellular electrodes [1] and the electrical breakdown phenomenon in the membranes of living cells have been the subject of extensive studies (e.g. [2–16]). Whilst these have included the dependence of the electrical breakdown on the pulse height, width and pulse repetition, many of these studies were performed using exponentially decaying pulses. This has complicated the interpretation and correlation of the results reported.

The exponentially decaying pulse[2] is used in many studies primarily because of the technical difficulties of producing pulse generators capable of generating square pulses with large pulse heights (~ 1 kV) capable of delivering the large currents which will flow in cell suspensions (tens of amperes).

A difficulty also arises in detecting the breakdown phenomenon itself. In studies in which the electrical conductance of the membrane itself can be directly measured, for instance by using intracellular electrodes [6] or in lipid bilayers [17], the breakdown phenomenon can be unequivocally seen in the voltage–current characteristics. The increased electrical conductance on electrical breakdown could also be discerned in flow cytometry studies using variable potentials applied to the flow orifice [18].

The release of haemoglobin or uptake of substances can also be used as an indicator of electrical breakdown. The major disadvantages in these methods are that:

(i) there is a delay in obtaining the information after the pulse is applied and
(ii) the environmental conditions of the erythrocytes are changed when the sample is subsequently transferred to the haemolysis measurement system.

Here we describe an experimental technique for characterising the electrical breakdown phenomenon in erythro-

---

* Corresponding author. Tel.: +61-2-9385-4583; fax: +61-2-9385-4484.

E-mail address: coster@unsw.edu.au (H.G.L. Coster).

[1] Current address: Department of Radiation Oncology, Royal North Shore Hospital, St. Leonards, NSW, 2065, Australia.

[2] The exponentially decaying pulse can be readily obtained by discharging a previously charged capacitor through the test chamber containing a suspension of the cells under investigation.

cytes in which the process can be monitored continuously. Experimental results are presented in which square voltage pulses were used with red blood cells (RBC) suspended in isotonic saline.

2. Experimental

The method developed was in essence to apply square voltage pulses to a suspension of erythrocytes (or RBC) and to continuously monitor haemoglobin released from the cells by using an optical transmission method of measurement.

2.1. The electrical breakdown test chamber

The test chamber allowed the application of voltage pulses and the continuous measurement of optical transmittance. A schematic of the test chamber is shown in Fig. 1. It consists of three parts. The central part contains the actual chamber holding the test solution. The chamber is made of plexiglass and is fitted with a red LED and two photodiodes. One of these is located in line with the LED to measure optical transmittance through the sample whilst the other is situated in a normal direction to measure light scattering and measures light scattered by the plexiglass chamber itself. The latter provided a means of normalising any variations in the light output, although in practice it was found that this was unnecessary. The two outer parts of the set-up have cylindrical plexiglass protrusions on which are mounted flat 8 mm diameter platinum electrodes. The protrusions fit into the cylindrical recesses in the central component to form the test cavity. This modular construction allowed the chamber to be readily dismantled to facilitate cleaning of the platinum electrodes and chamber.

To fill the chamber with the cell suspension, only one of the outer sections with the platinum electrodes was inserted

first, the chamber was then filled with the suspension of RBC in saline and the second outer section then pushed into place. Any excess solution was thereby expelled through a small outlet fluid hole (see Fig. 1) which was then sealed for the duration of the experiment. This procedure ensured that no air bubbles were trapped in the test chamber, which would give spurious light transmissions. At the concentration of cells used in the present experiments (∼ 0.3% by volume), normal Brownian motion substantially reduces the rate of sedimentation during the experiment, although control experiments (without the application of a voltage pulse) were performed for each blood sample examined.

In order to obviate the effect that multiple pulses might have on the breakdown characteristics, each sample was exposed to only a single pulse of electric field. To examine the effect of field strength and pulse length it was therefore necessary to repeat the procedure many times with samples taken from the same donor stock supply. To facilitate the data collection a number of identical chambers were constructed. The application of the pulses and the subsequent measurements of optical transmission were performed using a multiplexed analogue-to-digital converter connected to a computer, see Fig. 2. The entire set of chambers was housed in a light-tight box to reduce interference in the optical measurements from ambient light.

2.2. Square pulse generator

The square pulses were obtained by an electronic switching (on and off) of a high voltage (0–2 kV) power supply (Pacific Photometric Instruments 228). The electronic circuit built for this purpose was capable of producing pulses between 5 μs to 5 ms duration and delivered pulses up to 1 kV with currents of up to 25 A; see Appendix A for details. Generally, the pulse length used in the experiments did not exceed 50 μs. The switching
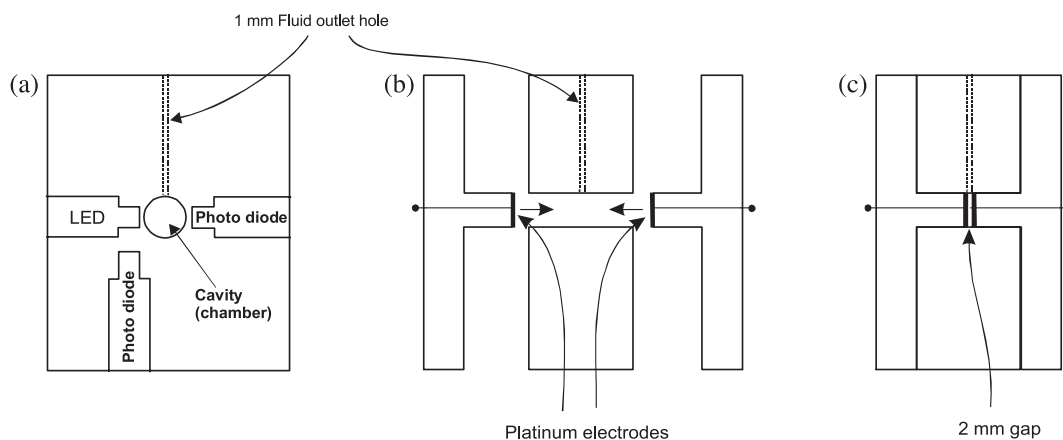

Fig. 1. A schematic diagram of the sample holder showing (a) a lateral view of the central plexiglass block designed to hold the photodiode–light emitting diode system, the sample (in the cavity) and the outlet fluid hole used for expulsion of excess liquid from the cavity; (b) an end elevation with each of the sections separated and; (c) an end elevation with each of the plexiglass sections fitted together.
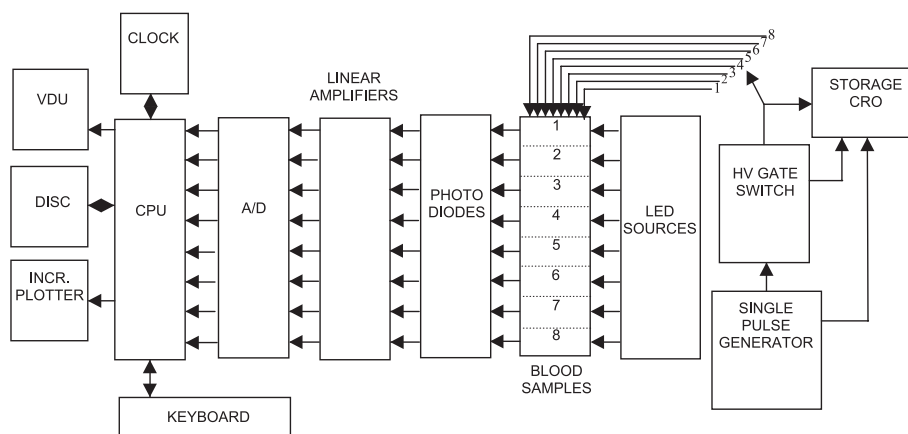
Fig. 2. Schematic diagram of the computer interfaced set-up.

circuit and technical details of the major components is shown in Fig. 13 of Appendix A. It is based on a fast turn-off thyristor (GTO) triggered by a MOSFET. The pulses applied across the blood sample were monitored on a storage oscilloscope (Hitachi model VC-6041(B)).

2.3. Optical transmission measurements

The suspended RBC in the isotonic saline solution appear as particles that cause random light scattering and the blood suspension (in isotonic saline) has a lower light transmission, for light in the wavelength range 400–600 nm, than a solution of isotonic saline. On electrical breakdown of the erythrocyte plasma membrane, some of the cells haemolyse; haemoglobin is released from the cells; and the light scattering from the remaining empty shells ("ghost cells") is greatly reduced. The released haemoglobin mixes with the isotonic saline to form a bright-red solution, that has a high transmittance to light in the wavelength range 400–600 nm. At least for dilute suspensions of RBC the increase in light transmission on cell haemolysis is directly proportional to the number of cells that haemolyse to form ghost cells. Thus for the concentration of suspended RBC in isotonic saline used in this procedure, the Lambert–Beer law describes the light absorbance as:

$$a = \varepsilon_\lambda CD \tag{1}$$

where a = absorbance; ε_λ = molar absorption coefficient at wavelength, λ (due to the combined effects of light scattered by the RBC and transmittance through the solute; C = RBC and solute concentration (moles per litre); D = path length (cm) of plexiglass cavity.

For the measurements using an LED light source and a photodiode detector, we can define an absorbance as:

$$a = \log_{10}\left(\frac{I + I_1' + I_2' + I_3'}{I_0 + I_1 + I_2 + I_3}\right) \tag{2}$$

where I_0 = photocurrent that would result from light incident to blood sample; I = photocurrent due to light transmitted to the photodiode; I_1, I_1' = photocurrent produced by stray scattered light; I_2, I_2' = additional offsets produced by the pre-amplifiers; I_3, I_3' = the diode dark current.

The light emitted from the LED on one side of the plexiglass block (see Fig. 1) passes through a 1 mm aperture to the photodiode on the other side. The small aperture ensures that the photodiode measuring the transmitted light through the sample is not exposed to any extent to light scattered from the plexiglass walls. The photodiode dark current produces an output signal of ~ 0.7 mV and, for the purposes of the study, was negligible. Eq. (2) with Eq. (1) therefore simplifies to the form:

$$\log_{10}\left(\frac{I}{I_0}\right) = -\varepsilon_\lambda CD \tag{3}$$

Thus,

$$\log_{10} I_0 - \log_{10} I \propto C \tag{4}$$

Ideally, the path length, D, and the molar absorption coefficient, ε_λ, should be constant so that the logarithmic ratio of the incident light to the transmitted light is proportional to the solute concentration or, in this case, the number of RBC scattering the transmitted light signal. In practice, this may not be correct for all cases. For example, if the size or shape of the RBC changes, then the scattering would change even when no haemolysis occurred.

The change in light intensity (Eq. (4)) measured as a function of RBC concentration is shown in Fig. 3. It is clear that the system gave a good linear relationship between cell concentration and light intensity. In a separate experiment, the transmitted light intensity was measured for 15 different blood samples ranging from 0.05% to 1.0% concentration for each of the eight experimental chambers. The maximum percent error (to two standard errors) for each of the blood sample holders over the range of sample concentrations
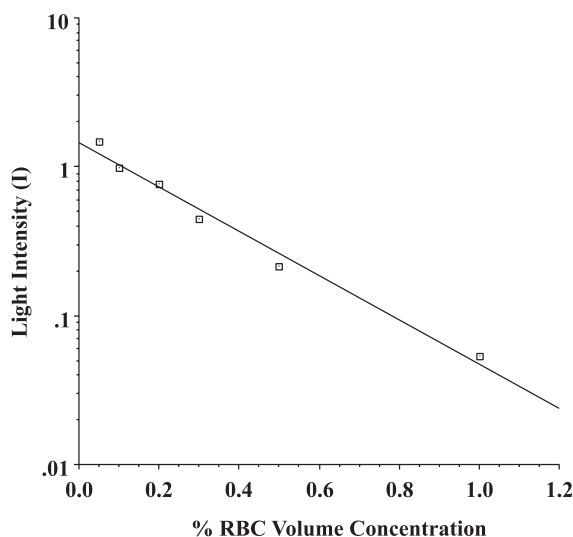
Fig. 3. The light intensity measured in the sample holder for a range of erythrocyte/isotonic saline concentrations from 0.05% to 1.0%. The slope of the line of best fit for each of the holders was similar with an overall mean of -1.653 ± 0.172.

used in the present study varied from 0.02% for the lowest blood concentration to 0.26% for the highest blood concentration. Since a maximum blood concentration of 0.3% was used for this work, the percent variation of the light transmission was expected to be better than 0.1%.

2.4. Erythrocyte preparations

Erythrocytes were obtained from fresh blood (less than 1 h after collection) and stored in lithium heparin sample tubes. The erythrocytes were separated from the plasma by centrifugation for 10 min at $1000 \times g$. The buffy coat (lymphocytes) were first removed using a Pasteur pipette. The erythrocytes were then washed three times by resuspension in isotonic saline followed by further centrifugation. Packed RBC (150 μl) were then dispensed into 50 ml of isotonic saline (to give an ∼ 0.3% volume concentration cell suspension) for the experiments.

2.5. Thermal effects

The volume of the cell suspension was 100 μl and hence the maximum temperature rise expected as a result of an 800 V pulse would be 0.2 °C for a 5 μs pulse and 2 °C for a 50 μs pulse. It has been shown that such temperature jumps do not in themselves cause haemolysis of erythrocytes [8].

3. Results

3.1. General

In the experiments, variables such as temperature, time after collection, plasma and protein content in the blood

were, wherever possible, either excluded or kept constant for all the investigations. The 0.3% RBC suspension under investigation were kept at a room temperature of 21 to 24 °C during the experiments.

After a series of 8 to 10 experiments, it was noted that a carbon-like material was deposited on the surface of the plexiglass chamber. These deposits appear to provide a conductive path for the current to flow around, rather than through, the suspended RBC solution. To avoid this, the chambers were thoroughly cleaned at frequent intervals.

3.2. Sedimentation of erythrocytes

Even when no pulse is applied to the sample, the transmitted red light signal gradually changes due to sedimentation under gravity. Over the 20-min interval for which measurements were generally performed the change in light transmission due to sedimentation was considered insignificant compared to the changes in light transmission due to haemolysis. The effect of sedimentation can be seen in the control experiments presented in Fig. 4. In these experiments no voltage pulses were applied to the electrodes.

It is worthwhile noting at this stage, that subtle differences in the shape of these sedimentation curves when no pulse is applied, occurred, probably due to changes in the morphology of the erythrocytes from their initial biconcave ellipsoidal shape.

In each experimental run, one of the chambers was used as a control (no pulse applied).

3.3. Data presentation

The experimental data on changes that occur over time when voltage pulses are applied to the sample will be
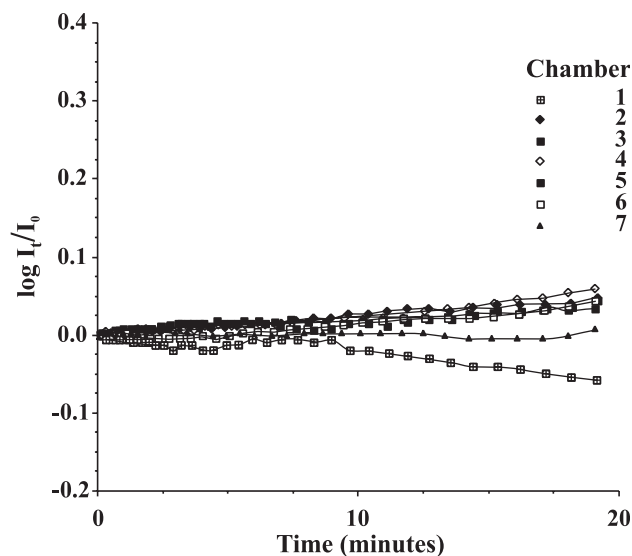

Fig. 4. A measurement of erythrocyte sedimentation recorded over a 20-min period with no voltage applied to each of the seven blood samples.

presented in terms of differences between the logarithm of the light intensity at a time $t = 0$, and the logarithm of the light intensity at time t (that is, $\log_{10}(I_t) - \log_{10}(I_0) = \log_{10}(I_t/I_0)$). With reference to Eq. (4), this measure should be directly proportional to the number of intact RBC scattering the red light that is passing through the sample. The measured light intensity could also vary due to a number of factors other than haemolysis, and so the results are expressed as the logarithm of light intensity relative to time zero rather than a percentage haemolysis.

3.4. Electrolysis effects

Before investigating the effects of an electrical pulse on the suspended RBC, the effects of hydrolysis needs be examined. When a large current flows through the sodium chloride solution, hydroxyl and hydrogen ions will be discharged at the electrodes and gas bubbles will collect on the electrodes. The red light from the LED reflected off the surface of the gas bubbles attached to the electrodes causing a reduction in the photodiode output. Figs. 5 and 6 illustrate the magnitude of electrolysis observed using 5 and 50 μs pulses of various pulse heights. The results presented in Fig. 5 shows that there was a threshold for electrolysis between 580 and 600 V for a 5 μs pulse. Residual effects of the electrolysis disappeared after about 10 min.

With pulse lengths of 50 μs, the hydrolysis effect was initially much more marked when the pulse height was in the range of 480–640 V. The reduced light intensity was a significant factor during approximately the first 2 min when the pulse was less than 600 V, 5 min for 600 V and 10 to 15 min for 640 V. It is concluded from this that if the haemolytic effects were studied at 20 min after the pulse
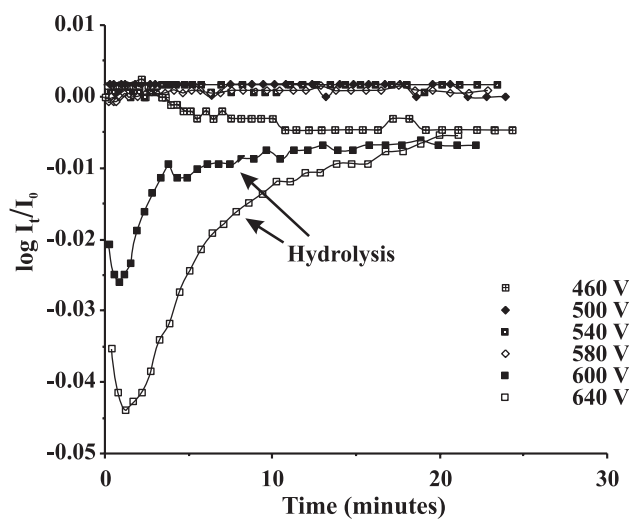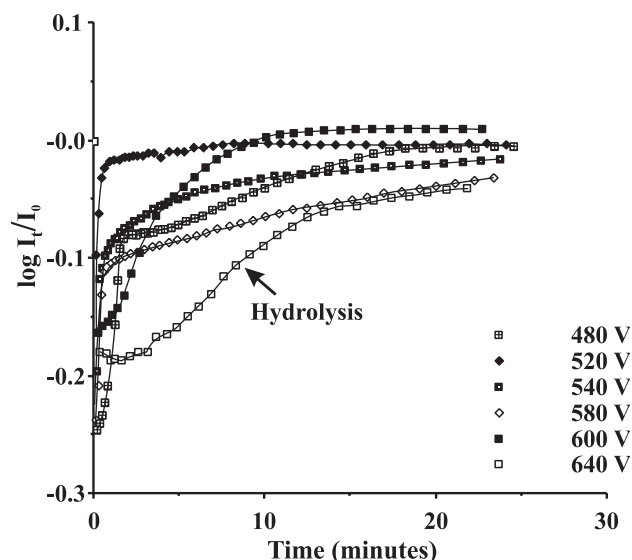

Fig. 6. Electrolysis caused by application of 50 μs pulses of various pulse heights in the range of 480–640 V in an isotonic saline solution.

was applied, the direct interference in the optical measurements due to electrolysis would be minimal.

Haemolysis causes an *increase* in optical transmittance, rather than a decrease, as is the case with electrolysis. Hence, the rapid increase in transmittance observed on electrical breakdown is not an artifact of the formation of bubbles.

3.5. Effect of pulse height on haemolysis

The form of the time curve of haemolysis depended in a complicated way on the pulse length and pulse height.

Fig. 7 illustrates the results obtained using 5 μs pulses of 0, 480, 500, 530, 560, 600 and 640 V applied to separate

Fig. 5. Electrolysis caused by the application of 5 μs pulses with various pulse heights in the range of 460–640 V applied across the electrodes in an isotonic saline solution.
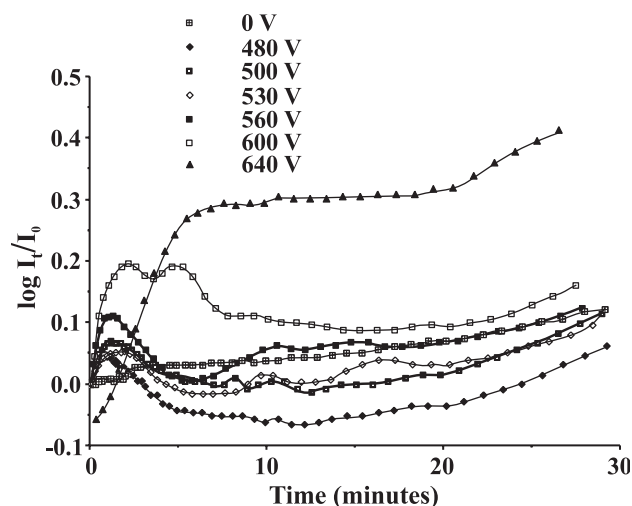

Fig. 7. The haemolytic curves obtained during a 30-min period using a 5 μs pulse and pulse heights of 0, 480, 500, 530, 560, 600 and 640 V.

samples of RBC suspensions. The control sample (results shown in Fig. 4) had an almost constant light transmission intensity but, at the lowest pulse voltage of 440 V applied, the light intensity following the pulse in this case, fell below the control curve, indicating an initial increase in light scattering (decrease in light transmission). On increasing the pulse height applied to the cell suspension to 480 V, a small peak in the light transmittance occurred in the early period of the curve followed by a decrease to less than the initial pre-pulse light transmission. The height of this initial peak progressively increased as the pulse voltage was increased up to 600 V. A distinct change in the curve then appeared at 640 V. At this pulse height there appeared a short initial decrease followed by a rapid, almost linear, increase in the light intensity before eventually leveling off to a plateau.

3.6. Critical voltage for haemolysis

The haemolytic curves for the same blood sample, recorded at 2, 4 and 12 h after collection, produced similar results (not shown). All of the haemolysis curves showed the distinct increase in the light transmission for pulses greater than 600 V. However, the detailed form of the haemolysis time courses were very varied and it was not possible to categorize these curves.

On the other hand, if the relative light intensity at a fixed time post-pulse is plotted as a function of the pulse height applied (or pulse length for a given constant pulse height), a consistent picture emerged. Fig. 8a is such a plot of light transmittance at 20 min post-pulse as a function of pulse height, taken from the haemolysis curves shown in Fig. 7. These results show the combination of data from two experiments obtained for 5 μs pulses at 2 and 4 h after blood collection. A sharp rise in haemolysis can be seen when the pulse height increased beyond $\sim$ 570 V for a single pulse applied to the sample. By separating the data into two groups representing the cell pre-breakdown and post-breakdown phase, a line of best fit could be computed for each of the two data series. The intercept between these two lines can now be used to define the "critical voltage", V_c.

Using this method to determine the critical breakdown voltage had an uncertainty of $\pm$ 5 V. In another experiment (not shown) the results obtained on a blood sample 12 h after collection, the average critical haemolysis voltage for breakdown using 5 μs pulses was then 565 V (Fig. 8b). The critical voltage of 570 V obtained from the first two experiments equates to a field strength of $\sim$ 304 kV/m (for the particular electrode separation used).

Similarly, the critical voltage for haemolysis using 50 μs pulse on the same blood sample was found to be 550 $\pm$ 5 V or a critical field strength of 292 kV/m.

A determination of the critical haemolysis voltage could also be deduced from the haemolysis data at various other times after the application of the pulses. In the sample blood
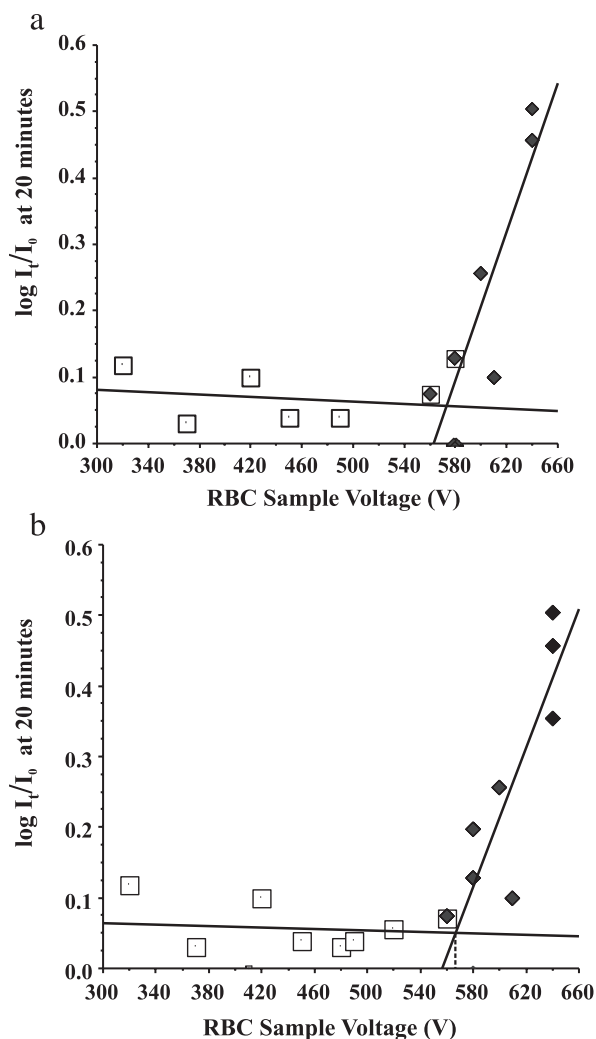

Fig. 8. (a) A plot of the logarithmic light intensity measured at 20 min after the 5 μs pulse subtracted by the logarithmic light intensity at time zero (log I_{20}/I_0) and plotted against the voltage applied to each blood sample. A critical voltage (V_c) of 570 $\pm$ 5 V (304 kV/m) was defined at the intercept between the two lines of best fit. The data from two experiments, obtained at 2 and 4 h after blood collection, were combined for this V_c result. (b) A critical voltage of 565 $\pm$ 5 V (300 kV/m) was obtained by combining a third set of 5 μs pulse data (to that shown in (a)) measured at 12 h after the initial blood collection from the donor.

shown in Table 1, the results so obtained at 5, 10 and 20 min after the application of pulses were very similar and were in the range 590 to 605 V. However, the fitting of the straight-line segments was more definitive for the data obtained 20 min after the application of the pulses.

3.7. Pulse length

For very short pulse lengths (nanoseconds), it has been reported [19] that the critical voltage for electrical breakdown of cell membranes is dependent on pulse length; the critical voltage decreases with increasing pulse length. However, the degree of haemolysis did not appear to be pulse length dependent in those studies.

Table 1
The critical voltage (V_c) determined at 5, 10 and 20 min after applying the 50 μs pulse are very similar

Exp. no.	Critical voltage (V_c)			Slope of haemolytic rise after critical RBC rupture		
	5 min	10 min	20 min	5 min	10 min	20 min
1	590	595	590	0.003	0.005	0.007
2	590	595	605	0.003	0.008	0.010
3	–	595	590	–	0.003	0.004
Average	590	595	595 ± 5	0.003	0.005	0.007

The average V_c in this example is 595 ± 5 V.

The electrical breakdown occurs at a fairly well defined electric potential difference, for a given pulse length. Using square pulses (that are of constant voltage) we investigated the effect of pulse length on the haemolysis.

At a fixed pulse height of 600 V, pulses of 10, 20, 40, 60, 80 and 100 μs duration were applied to the samples. Fig. 9 shows the resultant haemolysis curves so obtained. As the pulse length was increased in these experiments, the peak that appeared during the initial relative light transmission was reduced. The effect was masked by the increased incidence of electrolysis. An increase in the incidence of haemolysis for the longest pulse length also became apparent.

The relative light transmittance 20 min after the application of the pulses provides, as before, a clearer definition of the critical breakdown phenomenon. This is shown in Fig. 10 from which it follows that for a pulse height of 600 V, the critical pulse length for haemolysis, was 60 μs.

Repeats of these experiments for various pulse heights showed that the critical pulse length for haemolysis progressively increased with decreasing pulse height (Fig. 11). The relationship between the critical pulse length required for different pulse heights appeared to be linear; see Fig. 12.
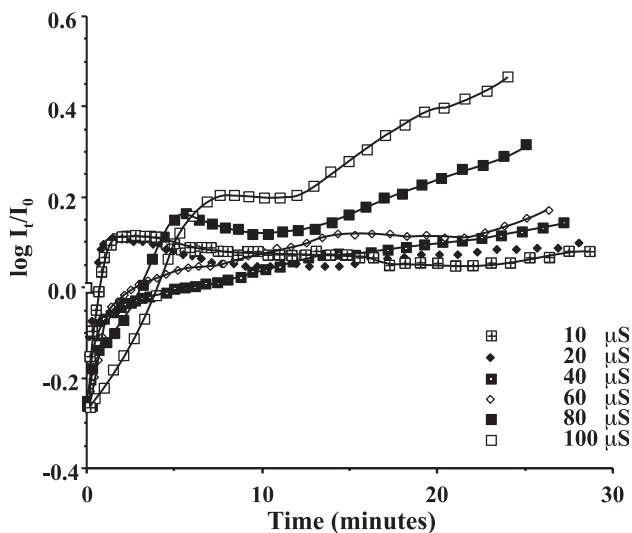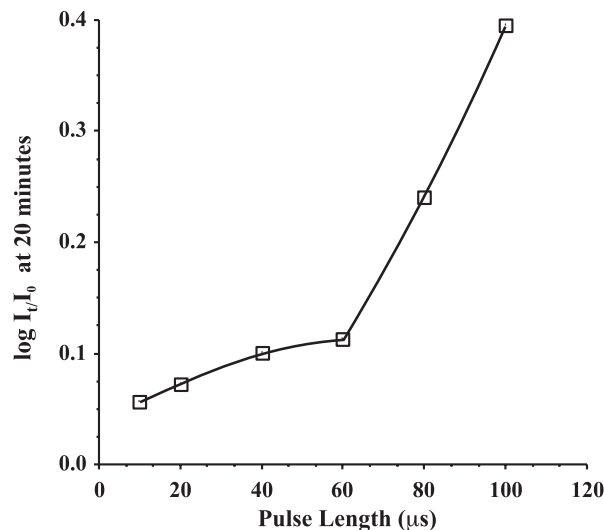

Fig. 10. A plot of the logarithmic light intensity measured at 20 min after 600 V pulses are applied subtracted by the logarithmic light intensity at time zero (log I_{20}/I_0) for a range of square wave pulse lengths. A sharp increase in this light intensity at 60 μs indicates the critical pulse length at which haemolysis occurs for a 600 V pulse.

3.8. Correlation of critical voltage with cholesterol levels in the blood

It is known that cholesterol has effects on the stability (increased [20,21]) and electrical conductance (decreased [22]) and capacitance (decreased [22]) of lipid bilayer membranes. We obtained cholesterol levels in the plasma of the blood samples used in the experiments to determine if there was any correlation between the critical breakdown parameters (pulse height and length) and the concentration of cholesterol in the plasma. No correlation between the critical voltage and the blood plasma cholesterol levels was found in these experiments. Similarly,

Fig. 9. The haemolytic curves obtained with a pulse of 600 V and pulse lengths of 10, 20, 40, 60, 80 and 100 μs.
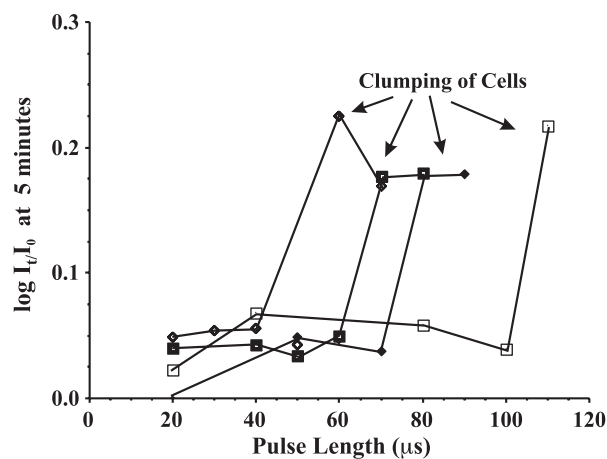

Fig. 11. The critical pulse length progressively decreased as the sample voltage was increased (data taken from a 5-min post-pulse haemolytic curve).
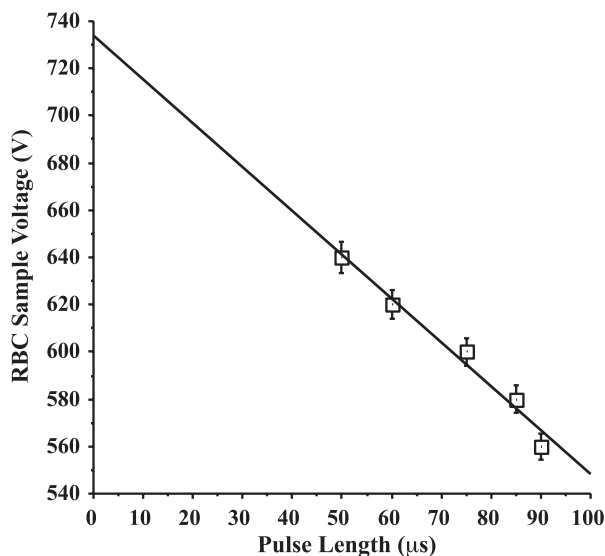
Fig. 12. A plot of the critical pulse length against pulse height applied to the RBC sample for a particular donor.

no correlation was found between the critical breakdown for haemolysis and the blood (cell) count for the samples from the various donors.

4. Discussion

The technique described for monitoring haemolytic events following the application of pulsed electric fields provides a reproducible method for determining the critical electric field strength for breakdown of erythrocytes. The critical field strength for haemolysis is dependent on pulse length, decreasing from 304 kV/m for 5 μs to 292 kV/m for 50 μs pulses (for one of the specific donors reported in this

paper). The values for the critical field strengths reported in the literature for erythrocytes are in the range 100 to 900 kV/m, obtained using various methods and various pulse waveforms—see Table 2.

Experiments on single cells with intracellular electrodes [6,23] and also on lipid bilayer membranes [17], suggest that the breakdown occurs at a critical, well defined, membrane potential difference. If the mechanism for electrical breakdown in erythrocytes occurs by a similar mechanism, then in experiments such as the one presented here, using a suspension of cells, the breakdown of the cell membrane would occur after the transmembrane potential of the erythrocytes had reached some critical value. The potential difference across the cell membrane, however, changes on application of the external field with a time constant, τ that is determined by the membrane capacitance and the conductivities of the cytoplasm and external solution. Typically, this time constant is of the order of 1 μs. For short pulses, of this duration therefore it would be expected that the pulsed field strengths required to take the membrane potential to the critical breakdown potential would decrease with increasing pulse lengths. For longer pulses of 10 μs or more, however, this would not be expected to be the case since there would then be sufficient time for the membrane to charge.

In the present study, even for pulses much longer than the time constant for charging the membrane capacitance, the critical field strength to induce haemolysis decreased with increasing pulse length. This would suggest that the haemolysis process, in which the cell becomes permeable to very large molecules, involves additional electromechanical processes following the initial electrical breakdown itself of the membrane.

The formation of pores in lipid bilayers is also thought to be associated with the stability of the membrane. Thus

Table 2
Some examples of experiments used to measure the erythrocyte (RBC) electrical membrane breakdown characteristics, using either exponentially decaying pulses (*) or square wave pulses (**)

Reference	Medium	Measurement of Hb release	Electrode separation (mm)	Field strength	Pulse length
Pilwat and Zimmermann [29]	RBC, NaCl, buffer and sucrose	Coulter Counter	–	10 kV/cm	40 μS*
Kinosita and Tsong [8]	RBC, NaCl, buffer and sucrose	Absorptiometry (410 nm)	2–10	up to 2.2 kV	50 nS–10 mS
Riemann et al. [30]	RBC, acid citrate and dextrose buffer	Spectrophotometer (398 nm)	10	12–14 kV/cm	5–10 μS*
Vieken et al. [31]	RBC, buffers I and II	Fixed and stained for electron microscope	–	12 kV/cm	40 μS*
Saleemuddin et al. [32]	RBC, buffers I and II	Absorptiometry (415 nm)	–	12–16 kV/cm	40 μS*
Zimmermann et al. [18]	RBC, buffers I and II	Coulter Counter	–	1.6–9 kV/cm (equivalent)	–
Mishra et al. [33]	RBC, buffers I and II	Spectrophotometer (540 nm)	10	–	80 μS*
Akerson and Mel [34]	RBC and buffer	Resistive pulse spectroscopy	–	1–1.8 kV/cm	–
Smith and Cleary [35]	Mouse lymphocytes and buffer	Potassium content by flame photometry	5	3 kV/cm	2 μS**
Bliss et al. [12]	RBC and buffer	Flow cytometer (488 nm)	–	8.8 kV/cm	50 μS**

it is theoretically predicted that when pores reach a critical size, the energy of forming the pores decreases with further increases in the pore radius [17,24,25]. This leads to an unstable condition in which the pores grow uncontrollably. Further, the critical pore size for membrane rupture, at least for pores smaller than a Debye length, decreases with increasing membrane potential [20]. Steroids such as cholesterol increase the energy cost of forming a pore and are found experimentally to increase the stability of lipid bilayers and decrease their electrical conductance [22]. If electrical breakdown in erythrocytes occurs via the formation of critical-sized pores in the lipid matrix of the cell membrane, it might be expected that cholesterol would affect the breakdown potential, as indeed has been demonstrated in studies on lipid bilayers containing cholesterol [26]. The present study found that the plasma cholesterol level did *not* affect the critical breakdown potential. This is in contrast to an earlier study, which found that the critical breakdown voltage for RBC incubated in the presence of cholesterol-rich liposomes increased [27]. It should be noted here that changes in the blood cholesterol level do not necessarily determine directly the cholesterol/phospholipid ratios in the plasma membrane of RBC, although they are correlated. Interestingly, it has been found that cation transport in human erythrocytes also do not correlate with total cholesterol [28]. Our present observation of a lack of effect of plasma cholesterol on the critical breakdown potential would support the notion that electrical breakdown in these cells occurs via some mechanism other than the formation of voltage dependent pores in the lipid bilayer of the RBC. One such mechanism is run-away electrostrictive processes in proteins (see for instance Ref. [7]).

Acknowledgements

Appendix A. High voltage switching circuit

A circuit diagram of the switching circuit constructed for the experiments described is shown in Fig. 13.
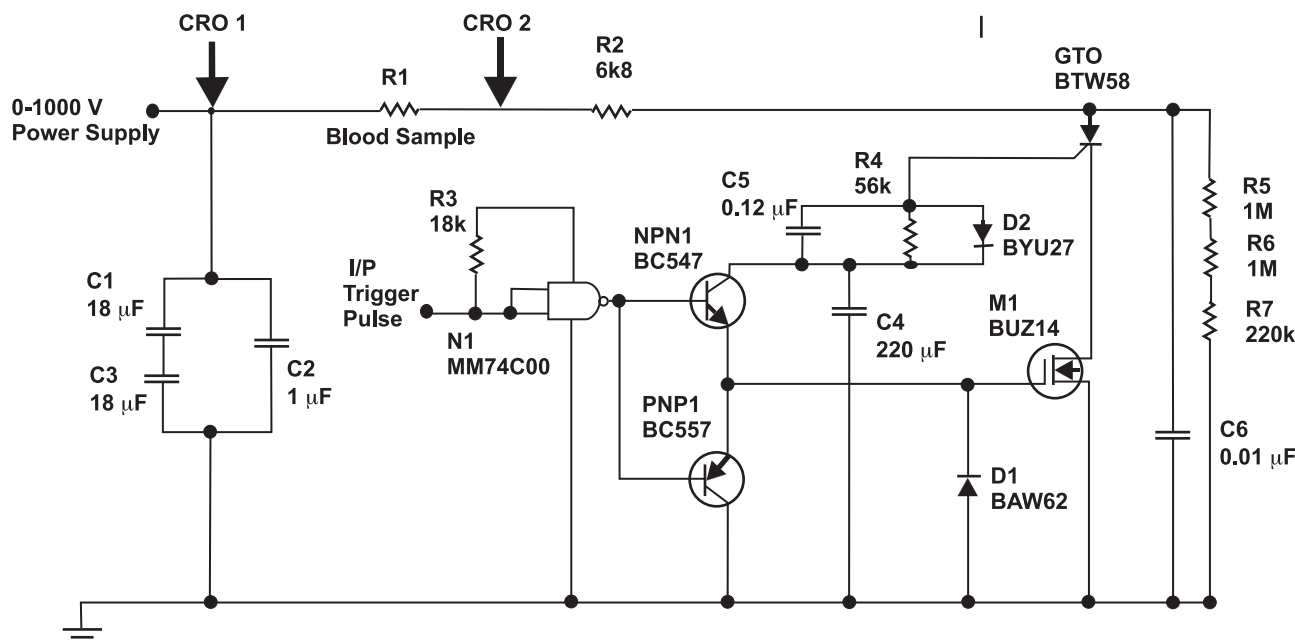

Fig. 13. The high voltage switching circuit. The input trigger pulse activates the MOSFET and GTO on and off, discharges the capacitors and applies an electric field across the erythrocyte suspension. The capacitors are not substantially discharged during the time that the switch is "on" so that the pulse height is essentially constant in time. The circuit is capable of providing pulses in the range between 5 μs to 5 ms in pulse length and up to 1 kV in height. By setting the desired voltage and pulse length, the circuit can deliver pulses with current flows of 25 A during the time the input trigger pulse is applied.

The positive output of the high voltage supply (Pacific Instruments, model 228) was connected in series with the GTO (thyrister BTW58-1500R)[3]. This acts as a normally open switch until a positive pulse is applied to the MOSFET (BUZ14)[4] transistor. The positive pulse closes the GTO gate allowing current to flow through the RBC suspension to earth until the trigger pulse falls to zero potential. This then turns off the MOSFET transistor and opens the gate on the GTO. The output of the high voltage supply was adjustable between 0 and 2 kV. The supply itself is current limited to 4 mA. For the present experiments, currents as high as 25 A were required and this was achieved by adding the capacitors across the high voltage supply as shown. During the time that the GTO is turned on, these capacitors discharge through the sample, which had a resistance of 27.6 Ω. The time constant for discharging these capacitors is therefore much longer than the maximum pulse length used in the present study and the pulse shape was determined entirely by the on and of switch circuit described above.

References

[1] H.G.L. Coster, A quantitative analysis of the voltage–current relationships of fixed charge membranes and the associated property of "punch-through", Biophys. J. 5 (1965) 669–686.

[2] A.J.H. Sale, W.A. Hamilton, Effects of high electric fields on microorganisms: I. Killing of bacteria and yeasts, Biochim. Biophys. Acta 148 (1967) 781–788.

[3] W.A. Hamilton, A.J.H. Sale, Effects of high electric fields on microorganisms: II. Mechanism of action of the lethal effect, Biochim. Biophys. Acta 148 (1967) 789–800.

[4] A.J.H. Sale, W.A. Hamilton, Effects of high electric fields on microorganisms: III. Lysis of erythrocytes and protoplasts, Biochim. Biophys. Acta 163 (1968) 37–43.

[5] A.E. Neumann, K. Rosenheck, Permeability changes induced by electric impulses in vesicular membranes, J. Membr. Biol. 10 (1972) 279–290.

[6] H.G.L. Coster, U. Zimmermann, Direct demonstration of dielectric breakdown in the membranes of *Valonia utricularis*, Z. Naturforsch. 30 (1975) 77–79.

[7] H.G.L. Coster, U. Zimmermann, The mechanism of electrical breakdown in the membranes of *Valonia utricularis*, J. Membr. Biol. 22 (1975) 73–90.

[8] K. Kinosita, T.Y. Tsong, Hemolysis of human erythrocytes by a transient electric field, Proc. Natl. Acad. Sci. 74 (1977) 1923–1927.

[9] G.K. Smith, S.F. Cleary, Dummy entry, Biochim. Biophys. Acta 763 (1983) 325–331.

[10] A.E. Sowers, Characterisation of electric field-induced fusion in erythrocyte ghost membranes, J. Cell Biol. 99 (1984) 1989–1996.

[11] L.V. Chernomordik, S.I. Sukharev, S.V. Popov, V.F. Pastushenko, A.V. Sokirko, I.G. Abidor, Y.A. Chizmadzhev, The electrical breakdown of cell and lipid membranes: the similarity of phenomenologies, Biochim. Biophys. Acta 902 (1987) 360–373.

[12] J.G. Bliss, G.I. Harrison, J.R. Mourant, K.T. Powell, J.C. Weaver, Electroporation: the population distribution of macromolecular uptake and shape changes in red blood cells following a single 50 ms square wave pulse, Bioelectrochem. Bioenerg. 20 (1988) 57–71.

[13] A.E. Sowers, in: A.E. Neumann, A.E. Sowers, C. Jordan (Eds.), The Mechanism of Electroporation and Electrofusion in Erythrocyte Membranes, Plenum, New York, 1989, pp. 229–256.

[14] D.A. Stenger, K.V. Kaler, S.W. Hui, Dipole interactions in electrofusion. Contributions of membrane potential and effective dipole interaction pressures, Biophys. J. 59 (1991) 1074–1084.

[15] V.L. Sukhorukov, H. Mussauer, U. Zimmermann, The effect of electrical deformation forces on the electropermeabilization of erythrocyte membranes in low- and high-conductivity media, J. Membr. Biol. 163 (1998) 235–245.

[16] M. Bier, W. Chen, T.R. Gowrishankar, R.D. Astumian, R.C. Lee, Resealing dynamics of a cell membrane after electroporation, Phys. Rev. E: Stat. Nonlinear Soft Matter Phys. 66 (2002) 6–11.

[17] L.V. Chernomordik, S.I. Sukharev, I.G. Abidor, Y.A. Chizmadzhev, Breakdown of lipid bilayer membranes in an electric field, Biochim. Biophys. Acta 736 (1983) 203–213.

[18] U. Zimmermann, G. Pilwat, F. Riemann, Dielectric breakdown of cell membranes, Biophys. J. 14 (1974) 881–899.

[19] R. Benz, O. Frohlich, P. Lager, M. Montal, U. Zimmermann, Pulse-length dependence of the electrical breakdown in lipid bilayer membranes, Biochim. Biophys. Acta 597 (1980) 637–642.

[20] H.G.L. Coster, Self-assembly, stability and the electrical characteristics of cell membranes, Aust. J. Phys. 52 (1999) 117–140.

[21] H.G.L. Coster, D.R. Laver, The effect of benzyl alcohol and cholesterol on the acyl chain order and alkane solubility of bimolecular phosphatidylcholine membranes, Biochim. Biophys. Acta 861 (1986) 406–412.

[22] C. Karolis, H.G.L. Coster, T.C. Chilcott, K.D. Barrow, Differential effects of cholesterol and oxidised cholesterol in egg lecithin bilayers, Biochim. Biophys. Acta 1368 (1998) 247–255.

[23] H.G.L. Coster, U. Zimmermann, Dielectric breakdown in the membranes of *Valonia utricularis*: the role of energy dissipation, Biochim. Biophys. Acta 382 (1975) 410–418.

[24] H.G.L. Coster, in: G.M. Eckert (Ed.), The Effect of Electric Fields on the Molecular Organisation and Pharmacological Response of Cell Membranes, CRC Press, Florida, 1990, pp. 139–150.

[25] Y.A. Chizmadzhev, V.B. Arakelyan, V.F. Pastushenko, Electric breakdown of bilayer lipid membranes: III. Analysis of possible mechanisms of defect origination, Bioelectrochem. Bioenerg. 6 (1979) 63–70.

[26] D. Needham, R.M. Hochmuth, Electromechanical permeabilization of lipid vesicles. Role of membrane tension and compressibility, Biophys. J. 55 (1989) 1001–1009.

[27] M.S. Goncharenko, I.I. Katkov, Effect of cholesterol on the stability of human erythrocyte membranes to electrical breakdown, Biofizika 30 (1985) 115–441.

[28] S. Hajem, T. Moreau, P. Hannaert, J. Lellouch, G. Orssaud, G. Huel, J.R. Claude, R.P. Garay, Erythrocyte cation transport systems and plasma lipids in a general male population, J. Hypertens. 8 (1990) 891–896.

[29] G. Pilwat, U. Zimmermann, Determination of intracellular conductivity from electrical breakdown measurements, Biochim. Biophys. Acta 820 (1985) 305–314.

[30] F. Riemann, U. Zimmermann, G. Pilwat, Release and uptake of haemoglobin and ions in red blood cells induced by dielectric breakdown, Biochim. Biophys. Acta 394 (1975) 449–462.

[31] J. Vieken, E. Jeltsch, U. Zimmermann, Penetration and entrapment of large particles in erythrocytes by electrical breakdown techniques, Cytobiology 17 (1978) 182–196.

---

[3] The BTW58-1500R thyrister has a repetitive peak off state voltage of 1500 V, a controllable anode current of 25 A, an average on-state current of 6.5 A and a turn-off fall time of 250 ns.

[4] The BUZ14 MOSFET has a drain-source voltage of 50 V, a drain current of 39 A and a total power dissipation of 125 W. The turn-off fall time is 200 ns.

[32] M. Saleemuddin, U. Zimmermmann, B.F. Schneewei, Preparation of human erythrocyte ghosts in isotonic solution: haemoglobin content and polypeptide composition, Z. Naturforsch. 32c (1977) 627–631.

[33] K.P. Mishra, L.D. Binh, B.B. Singh, Effect of dielectric discharge on drug treated mammalian cells, Indian J. Exp. Biol. 19 (1981) 520–523.

[34] S.P. Akerson, H.C. Mel, Osmotic hemolysis and fragility, a new model based on membrane disruption, and a potential clinical test, Biochim. Biophys. Acta 718 (1982) 201–221.

[35] G.K. Smith, S.F. Cleary, Effects of pulsed electric fields on mouse spleen lymphocytes in vitro, Biochim. Biophys. Acta 763 (1983) 325–331.